

# Recycling Ultrathin Catalyst Layers for Multiple Single-Walled Carbon Nanotube Array Regrowth Cycles and Selectivity in Catalyst Activation

Cary L. Pint,<sup>†,‡,||</sup> Nolan Nicholas,<sup>†,||</sup> Juan G. Duque,<sup>§,||</sup> A. Nicholas G. Parra-Vasquez,<sup>§,||</sup> Matteo Pasquali,<sup>‡,§,||</sup> and Robert Hauge<sup>\*,†,‡,||</sup>

Department of Physics, Chemistry, and Chemical and Biomolecular Engineering, and Richard E. Smalley Institute for Nanoscale Science and Technology, Rice University, Houston, Texas 77005

Received November 20, 2008. Revised Manuscript Received February 25, 2009

We utilize chemical vapor deposition to demonstrate the reactivation of catalyst for multiple regrowths of vertically aligned carbon nanotube arrays (carpets) in the context of water-assisted supergrowth. The carpets are transferred from the growth substrate, and the catalyst and substrate are reactivated by annealing in air. Annealing parameters control the length and diameter distribution of nanotubes in the regrown carpets due to active catalyst termination followed by a size-dependent process of iron carbide particle reoxidation. The lack of achieving indefinite regrowth from a 0.5 nm thick Fe layer can be attributed to factors such as catalyst dynamics taking place during the growth and regrowth processes.

## Introduction

The growth of aligned carbon nanotubes on solid substrates has been a topic of key interest in recent years.<sup>1,2</sup> The growth of densely packed arrays of aligned nanotubes eliminates the dependence on postgrowth processing for nanotube alignment and introduces a material that can be directly implemented into new technological applications, where nanotube density and alignment are key features of the desired material. In addition, the physical properties of single-walled carbon nanotubes (SWNTs),<sup>3,4</sup> including electrical<sup>5</sup> and thermal<sup>6</sup> conductivity and mechanical strength,<sup>7</sup> have made the synthesis of aligned SWNT films even more attractive from the standpoint of nanotechnology-based applications.<sup>8</sup> The versatility needed for such applications is apparent in growth of aligned structures of SWNTs, as aligned SWNTs have recently been demonstrated to grow both perpendicular<sup>9,10</sup> and parallel<sup>11</sup> to substrates. Applications based on nanotubes grown in aligned structures have

rapidly developed in the past few years and include supercapacitors,<sup>12</sup> adhesive tapes,<sup>13–15</sup> and membrane filters<sup>16</sup> among many others. As these applications develop, the bottleneck for their large-scale implementation will be based upon the limitations imposed at the growth stage.

Currently, the fundamental research drivers in carbon nanotube growth reflect the movement toward scalable processes for the production of large amounts of aligned SWNT material and processes that can yield reasonable control of the nanotube diameter and chirality for specific SWNT-based applications (chiefly in electronics). The downfall in the process of vertical array SWNT (carpet) growth is that there is no reasonable level of control on the selectivity. Particularly in the case of “supergrowth,” which is carpet growth assisted by the presence of a small amount of H<sub>2</sub>O, the nucleation density is very high, but the SWNTs have diameters often ranging up to 4 nm or more. For many applications, this wide range of high-quality SWNT material having a broad diameter distribution is acceptable, in which case one will seek to optimize the amount of growth that can possibly be achieved by an ultrathin catalyst layer. However, this broad diameter range is unacceptable for many other applications which require a reasonable level of control on the range of SWNT diameters. As a result, sacrificing an

\* Corresponding author. E-mail: Hauge@rice.edu.

† Department of Physics.

‡ Department of Chemistry.

§ Department of Chemical and Biomolecular Engineering.

|| Richard E. Smalley Institute for Nanoscale Science and Technology.

- (1) Ren, Z. F.; Huang, Z. P.; Xu, J. W.; Wang, J. H.; Bush, P.; Siegal, M. P.; Provencio, P. N. *Science* **1998**, 282, 1105.
- (2) Fan, S.; Chapline, M. G.; Franklin, N. R.; Tombler, T. W.; Cassell, A. M.; Dai, H. *Science* **1999**, 283, 512.
- (3) Ebbesen, T. W.; Ajayan, P. M. *Nature (London)* **1992**, 358, 220.
- (4) Bethune, D. S.; Klang, C. H.; de Vries, M. S.; Gorman, G.; Savoy, R.; Vazquez, J.; Beyers, R. *Nature (London)* **1993**, 363, 605.
- (5) Tans, S. J.; Devoret, M. H.; Dai, H.; Thess, A.; Smalley, R. E.; Geerlings, L. J.; Dekker, C. *Nature (London)* **1997**, 386, 474.
- (6) Che, J. W.; Cagin, T.; Goddard, W. A. *Nanotechnology* **2000**, 11, 65.
- (7) Yu, M. F.; Files, B. S.; Arepalli, S.; Ruoff, R. S. *Phys. Rev. Lett.* **2000**, 84, 5552.
- (8) Milne, W. I.; Teo, K. B. K.; Minoux, E.; Groening, O.; Gangloff, L.; Hudanski, L.; Schnell, J.-P.; Dieumegard, D.; Peauger, F.; Bu, I. Y. Y.; Bell, M. S.; Legagneux, P.; Hasko, G.; Amarasingha, G. A. J. *J. Vac. Sci. Technol. B* **2006**, 24, 345.
- (9) Hata, K.; Futaba, D. N.; Mizuno, K.; Namai, T.; Yumura, M.; Iijima, S. *Science* **2004**, 306, 1362.

- (10) Murakami, Y.; Chiashi, S.; Miyauchi, Y.; Hu, M.; Ogura, M.; Okubo, T.; Maruyama, S. *Chem. Phys. Lett.* **2004**, 385, 298.
- (11) Huang, S.; Cai, X.; Liu, J. *J. Am. Chem. Soc.* **2003**, 125, 5636.
- (12) Futaba, D. N.; Hata, K.; Yamada, T.; Hiraoka, T.; Hayamizu, Y.; Kakudate, Y.; Tanakie, O.; Hatori, H.; Yumura, M.; Iijima, S. *Nat. Mater.* **2006**, 5, 987.
- (13) Ge, L.; Sethi, S.; Ci, L.; Ajayan, P. M.; Dhinojwala, A. *Proc. Natl. Acad. Sci. U.S.A.* **2007**, 104, 10792.
- (14) Qu, L.; Dai, L. *Adv. Mater.* **2007**, 19, 3844.
- (15) Sethi, S.; Ge, L.; Ci, L.; Ajayan, P. M.; Dhinojwala, A. *Nano Lett.* **2008**, 8, 822.
- (16) Majumder, M.; Chopra, N.; Andrews, R.; Hinds, B. J. *Nature (London)* **2005**, 438, 44.

ultra-high yield only to activate catalyst particles in a specific diameter range is of significant importance in this case.

In this study, we present a new technique for achieving size control of the activated catalyst species and emphasize a method by which a catalyst layer can be recycled for multiple growth cycles while still retaining a high enough catalyst particle density to support carpet growth. The concept of this work is based upon the fact that the catalyst remains pinned to the supporting layer during the growth process. Recent work by Li et al.<sup>17</sup> and Iwasaki et al.<sup>18</sup> both indicated that thick multiwalled and single-walled carbon nanotube layers can be formed by re-exposing the catalyst layer to the carbon feedstock source at high temperature. In the case of layered SWNT array growth,<sup>18</sup> cooling the first layer in the plasma-enhanced chemical vapor deposition system prior to renucleation results in the formation of a capped SWNT in the second layer. This emphasizes that more than one growth is possible from the standpoint of removing and inserting the sample. Furthermore, Chiu et al.<sup>19</sup> recently demonstrated the ability to regrow a vertically aligned multiwalled carbon nanotube array multiple times using thick (3 nm) layers of Fe catalyst. Here, these authors discuss the ability to achieve high CNT quality following multiple growths from the same catalyst, emphasizing the loss of catalyst material occurring in the regrowth process. This further bolsters the motivation of our study, which is aimed at preserving the nature and morphological characteristics of the ultrathin (0.5 nm) layer of Fe catalyst to support multiple cycles of the highly efficient “supergrowth” process.

Therefore, the goal in the work presented here is twofold. In the first case, we present a technique by which regrowth can be achieved from an ultrathin catalyst layer (0.5 nm thick) and emphasize that an intermediate step to achieve catalyst reactivation can be utilized to result in a reasonable level of selectivity in the catalyst activation process. Second, we demonstrate our ability to recycle a 0.5 nm thick Fe catalyst layer to support SWNT carpet growth up to six times. Each time, the SWNT carpet is removed from the growth substrate and the catalyst is successfully reactivated for an additional growth period. This work demonstrates that the same process can lead to a highly recyclable or selective growth process, depending on the specific treatment for reactivation.

## Experimental Section

In this study, carpets were grown in a rapid insertion hot filament chemical vapor deposition apparatus,<sup>20–22</sup> where atomic hydrogen is created with a hot tungsten filament to reduce the Fe catalyst

- (17) Li, X.; Cao, A.; Jung, Y. J.; Vajtai, R.; Ajayan, P. M. *Nano Lett.* **2005**, *2*, 1997.
- (18) Iwasaki, T.; Robertson, J.; Kawarada, H. *Nano Lett.* **2008**, *8*, 886.
- (19) Chiu, C.-C.; Yoshimura, M.; Ueda, K. *Jpn. J. Appl. Phys.* **2008**, *47*, 1952.
- (20) Xu, Y. Q.; Flor, E.; Schmidt, H.; Smalley, R. E.; Hauge, R. H. *Appl. Phys. Lett.* **2006**, *89*, 123116.
- (21) Pint, C. L.; Nicholas, N.; Pheasant, S. T.; Duque, J. G.; Parra-Vasquez, A. N. G.; Eres, G.; Pasquali, M.; Hauge, R. H. *J. Phys. Chem. C* **2008**, *112*, 14041.
- (22) Pint, C. L.; Pheasant, S. T.; Pasquali, M.; Coulter, K. E.; Schmidt, H. K.; Hauge, R. H. *Nano Lett.* **2008**, *8*, 1879.

quickly for efficient SWNT carpet growth. With use of water-assisted (“supergrowth”) conditions with C<sub>2</sub>H<sub>2</sub> decomposition, a typical carpet having height between 600 and 700  $\mu\text{m}$  was obtained in 30 min at a reaction pressure of 25 Torr. This length was preferable for studying the yield in regrowth since measurement errors in carpet densities and carpet heights were minimal. To investigate the regrowth, a carpet was grown on a large chip ( $\sim$ 1.5 cm wide and 4 cm long) and broken into two pieces, having dimensions of approximately 0.5  $\times$  4 cm and 1  $\times$  4 cm. The smaller piece was studied via scanning electron microscopy (SEM) and optical spectroscopy, and the other was utilized for the second growth. To remove the carpet for a second growth, the carpet is removed from the substrate by pressing a piece of adhesive material onto the top of the carpet and then removing it. This process works with a range of adhesives, including carbon, Scotch, or Teflon tape, even though this technique seemed to be ineffective for removing the second carpet growth. To achieve multiple regrowths, we utilized the H<sub>2</sub>O etch process following growth<sup>23</sup> that was recently developed to free the strong metal–carbon bonds which form during cooling when the SWNT remains attached to the catalyst particle. In these cases, the growth was carried out at lower pressures (1.4 Torr) due to the optimization of the etch process for this low-pressure condition, and the uniformity of the length was measured through the electrical resistivity of the transferred film with an Alessa four-point probe in three identical spots in each case. This is necessary due to the impractical nature of breaking multiple pieces to study from the same growth substrate in a consistent way. It should be noted that, in all cases, the “regrowth” is carried out under conditions identical to those of the first growth.

## Results and Discussion

In the first studies carried out, the carpet was removed from the growth substrate and immediately placed back into the reaction gas flow for a second growth period, with no reactivation step. When this was performed, a low yield in regrown SWNTs is achieved, with mats of SWNTs between 2 and 3% of the height of the original carpet ( $\sim$ 13  $\mu\text{m}$ ) formed in identical growth conditions. This led us to consider the different ways in which better regrowth could be achieved. To begin, three different methods were considered for catalyst reactivation via oxidation: ultraviolet (UV) ozonization, brief oxygen plasma treatment, and annealing in the presence of air. We observed that the best regrowth took place after annealing in air, even though we were able to achieve up to 10% regrowth by ozone/UV treatment, and always less than 2% regrowth with brief oxygen plasma treatments (no better than not treating the catalyst layer). This allowed us to search for the optimum catalyst reactivation conditions by changing both the annealing time and temperature of the chip in the presence of air. The results of these experiments are presented in Figure 1, as the percentage of regrowth is plotted as a function of annealing temperature and time. It should be noted that to account for slight inconsistencies in carpet growth from one case to the next, the first and second growth were measured independently for comparison. For each data point, the regrowth reported is averaged over several height measurements taken through SEM. Figure 1a illustrates the percentage of regrowth as a function of temperature, when the exposure time at that

- (23) Pint, C. L.; Xu, Y. Q.; Pasquali, M.; Hauge, R. H. *ACS Nano* **2008**, *2*, 1871.

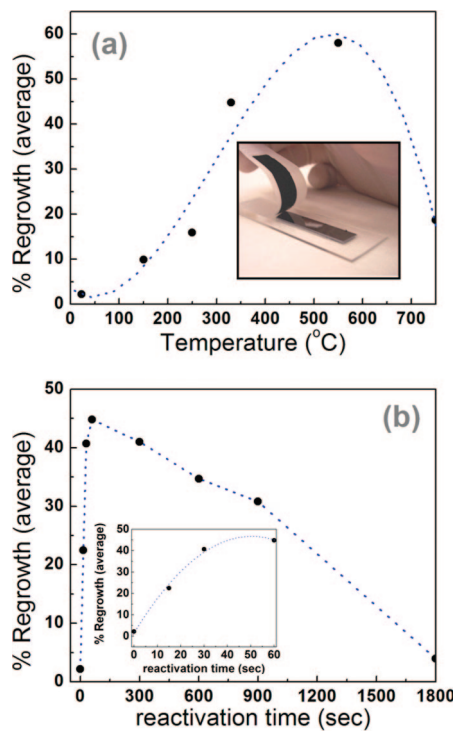


**Figure 1.** (a) Percentage of regrowth, measured by comparing the average heights of first and second growth, as a function of both (a) temperature, with 1 min exposure time, and (b) exposure time, at 330 °C. Inset in (a) is an image of a carpet being removed from a Si chip, and inset in (b) is a close-up view of the percentage of regrowth in the first 60 s of reactivation time, with a quadratic fit.

temperature is 1 min. The inset image illustrates the clean removal of the carpet from the growth substrate with an adhesive. Although full regrowth was never achieved, it should be noted that, at 550 °C for 1 min, the part of the growth substrate nearest to the tungsten hot filament had carpet heights that were comparable to that of the first growth (~85%). However, the carpet height was nonuniform, with heights further away from the hot filament of only about 50% of the height of the first growth, so that the average regrowth was only 58%. It should be noted that uniformity would be achieved if one reduced the size of the substrate or decreased the pressure, even though the substrates utilized in this study were large (4 cm long), and the diffusion distance of atomic hydrogen produced by the hot filament is short compared to this distance. After the annealing temperature is increased past 550 °C, the average regrowth is observed to decrease. A similar trend is also evident in the percentage of regrowth as a function of reactivation time shown in Figure 1b, where longer than 1 min of high-temperature exposure in air results in a decreased percentage of regrowth following a linear trend with time. This suggests that there are two competing effects that control the optimization of regrowth. The first must be the oxidation and reactivation of catalyst particles. Since the solubility of carbon in Fe decreases as the temperature decreases,<sup>24</sup> the particles likely solidify in a Fe<sub>3</sub>C or similar carbide state that is likely coated with a carbon outer shell. Therefore, to regrow, the carbon shell around the catalyst must be broken

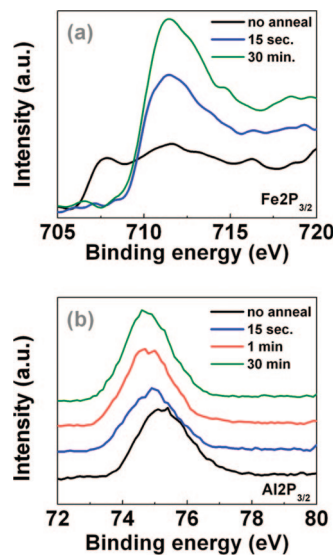


**Figure 2.** X-ray photoelectron spectroscopy binding energies for (a) Fe 2p<sub>3/2</sub> electrons and (b) Al 2p<sub>3/2</sub> electrons, after transfer of the carpet off the growth substrate and exposure to air at 330 °C for different amounts of time.

and the catalyst itself converted from an iron carbide to an iron oxide state for another reduction cycle. This process is similar to that required in HiPCO to expose and etch the catalyst.<sup>25</sup> Next, there seems to be a “poisoning” effect due to the alumina substrate when the reactivation temperature is raised too high. This could be a ripening effect of Fe–O into the bulk of the alumina, which is a thermodynamically available state since an e-beamed alumina layer will be relatively porous. This general picture describing these two competing effects is confirmed by X-ray photoelectron spectroscopy data, shown in Figure 2. This data is relative to a charge reference of adventitious carbon with a binding energy of 285.0 eV. First, the Fe 2p<sub>3/2</sub> spectra for a regrowth substrate where the carpet is removed with no intermediate annealing step has a binding energy peak well fit to a Gaussian with a center of 707.8 eV. This peak position is too low in binding energy to correspond to an oxide state of Fe, as such peaks are above 710 eV, in general. Instead, this peak is closer to that for metallic Fe (707.1 eV), and seems to be closest to the binding energy determined for Fe in an iron carbide compound.<sup>26</sup> However, only 15 s of annealing in air at 330 °C transforms the catalyst back into Fe<sub>2</sub>O<sub>3</sub>, with a binding energy in the range of 711 eV.<sup>27</sup> Next, the Al 2p<sub>3/2</sub> spectra shown in Figure 2b in the case of no intermediate annealing step indicates a binding energy peak position for Al of 75.3 eV. As the annealing time is increased, an evident shift in binding energy takes place and peak positions shift toward lower energies, with Gaussian centers at 74.91 eV (15 s), 74.77 eV (1 min), and 74.65 eV (30 min), with the fwhm constant at 1.7 eV, yielding a good fit in each case. This consistent trend in electron binding energies can be representative of a difference in the state of the Al<sub>2</sub>O<sub>3</sub>. The

(24) *Binary Alloy Phase Diagrams*; ASM International: Materials Park, OH, 2008.

(25) Xu, Y. Q.; Peng, H.; Hauge, R. H.; Smalley, R. E. *Nano Lett.* **2005**, 5, 163.

(26) Shabanova, I. N.; Trapeznikov, V. A. *J. Electron Spectrosc. Relat. Phenom.* **1975**, 6, 297.

(27) Olefjord, I.; Mathieu, H. J.; Marcus, P. *Surf. Interface Anal.* **1990**, 15, 681.

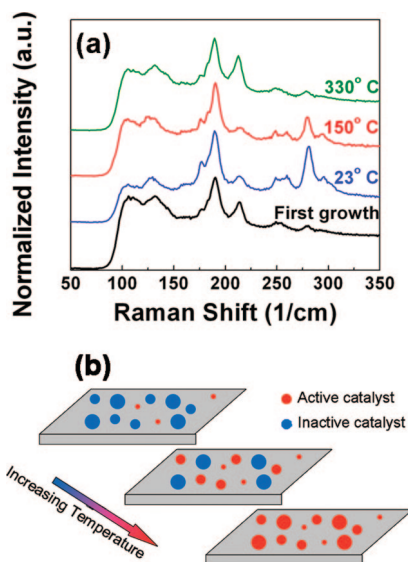


**Figure 3.** (a) SWNT radial breathing modes from polarized Raman spectroscopy, with the light polarization parallel to the carpet alignment. Measurements were taken with a 633 nm laser for carpets regrown under 1 min of exposure to air at temperatures ranging between 23 and 330 °C. (b) Illustration showing the concept of the catalyst particle size dependence in the thermal reactivation process.

peak position after a 30 min anneal probably represents a restructuring of the  $\text{Al}_2\text{O}_3$  layer into a near fully dense crystal structure that is closer to bulk  $\text{Al}_2\text{O}_3$ , whose binding energy is at about 74.7 eV.<sup>28</sup> It is likely that, during this process, Fe–O will also slowly ripen into the structure of the  $\text{Al}_2\text{O}_3$ , creating a mixed metal oxide that is a thermodynamically stable configuration. Although this remains to be completely determined from a detailed experimental perspective, it is evident for this study that the inability to regrow from a recycled catalyst layer is tied to this difference in chemical identity of the alumina.

In addition to the ability to regrow a significant percentage of carbon nanotubes produced in the first growth—which is attractive from the standpoint of production—it is also of interest to us to have control over the nanotube diameters grown in the carpet. Such control is desirable in carpets because they are already grown in a dense, aligned configuration that is highly attractive for many applications. However, the inability to control the diameter distribution makes this growth technique unattractive to many applications, such as membrane filtration for water desalination,<sup>29</sup> where diameter control is a highly important factor. In this work, we employed both Raman and fluorescence spectroscopy to monitor the diameters of regrown SWNTs, in addition to measurements of SWNT carpet density. Size selectivity in second growth is apparent in Raman spectra of SWNT radial breathing modes (RBM), shown in Figure 3. For these measurements, a 633 nm laser, with the electric field parallel to the direction of carpet alignment, was focused on the side of as-grown carpets. The spectra shown in Figure 3 are then normalized to the RBM located at  $180\text{ cm}^{-1}$ , which has the dominant signal in each case. It is evident that the

diameter distribution of SWNTs in carpets grown before peeling is mostly populated by larger diameter nanotubes, with RBMs at frequencies lower than  $220\text{ cm}^{-1}$ , corresponding to SWNTs with diameters larger than about 1 nm. After peeling and exposure of the catalyst to air at room temperature, the RBMs located at higher frequencies (between 245 and  $270\text{ cm}^{-1}$ , with diameters in the range of 0.82–0.91 nm) appear, indicating a significantly larger percentage of smaller diameter nanotubes grown in the carpet. As the temperature of heat treatment in air increases, the relative intensity of the RBMs in the range of 245– $270\text{ cm}^{-1}$  decreases and the breathing modes at low frequencies, around  $100\text{--}150\text{ cm}^{-1}$ , once again appear. When the heat treatment temperature is increased to 330 °C and above, the RBMs look almost identical to that observed in the first growth, indicating that size selectivity is lost by reactivating catalytic particles of all sizes. It should be noted that the presence of large nanotubes is suggested by the broad RBM peak in the Raman spectra located close to the low-frequency filter at  $100\text{ cm}^{-1}$  and is consistent with TEM measurements on material typically grown by this technique. It should be also noted that the G/D ratio for the sample reactivated by just room temperature treatment in air (23 °C in Figure 3) was  $\sim 12$ , indicating a defect-free SWNT population in this case. The G/D ratio for the as-grown sample was  $\sim 3$ , and the G/D ratio for the carpet grown from the catalyst layer reactivated by annealing at 330 °C was  $\sim 3.5$ . The low G/D ratio is typically indicative of some nanotubes having between 2 and 4 walls (<25% in TEM) that grow under conditions of elevated pressures (25 Torr), which was the case for this study.

In addition to Raman spectroscopy, photoluminescence (PL) spectroscopy is another secondary tool for characterizing diameter-dependent properties of semiconducting (typically about two-thirds of the total population) single-walled carbon nanotubes.<sup>30</sup> PL measurements, shown in Figure 4, were carried out on solutions of regrown carpets suspended in 1 wt % sodium deoxycholate solution, after 1 h of bath sonication and 20 min of tip sonication at 38% amplitude. Since it is evident in the Raman spectra that the effects of annealing are most evident in the population of small diameter SWNTs, PL offers insight into the relative constituents of this population. The intensities in Figure 4 are normalized to the peak for a (7,5) SWNT, which indicates the relative ratios of larger and smaller SWNTs in the solutions. Consistent with the results obtained by Raman spectroscopy, the relative PL intensities of the larger diameter SWNTs in the spectra increase with the elevated annealing temperature up to 330 °C and stay relatively constant at higher temperatures. This is apparent by noting the relative intensities of the two largest peaks in the 785 spectra, the (10,5) peak and the (9,7) peak with emissions at  $\sim 1270$  and  $1340\text{ nm}$ , respectively. This again suggests the same size dependence of the reactivation process, where thermal energy in an oxygen-rich environment (air) allows activation of only a certain distribution of particle sizes, determined by the annealing temperature. However, between 330 and 550 °C,

(28) Moulder, J. F.; Stickle, W. F.; Sobol, P. E.; Bomben, K. D. *Handbook of X-ray Photoelectron Spectroscopy*; Physical Electronics, Inc.: Eden Prairie, MN, 1995.

(29) Corry, B. *J. Phys. Chem. B* **2008**, *112*, 1427.

(30) Bachilo, S. M.; Strano, M. S.; Kittrell, C.; Hauge, R. H.; Smalley, R. E.; Weisman, R. B. *Science* **2002**, *298*, 2361.

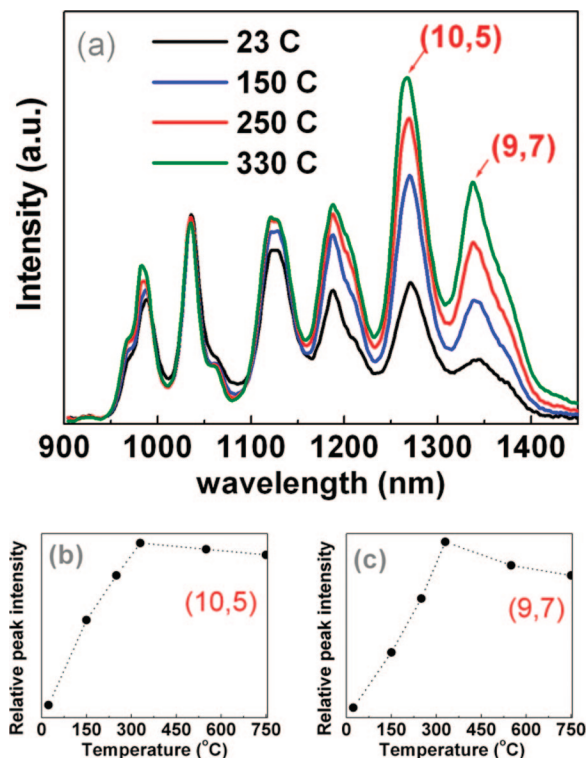


**Figure 4.** (a) Relative fluorescence emission spectra from surfactant-suspended, regrown carpets with air exposure at temperatures between 23 and 330 °C, excited with a 785 nm diode laser. Intensities are normalized to the peak for a (7,5) SWNT to emphasize the relative intensity of larger fluorescent tubes as a function of annealing temperature. Numbers on the y-axis are relative to data in the 660 nm fluorescence spectrum (not shown). (b) and (c) Relative peak intensities for the (10,5) and (9,7) nanotubes as a function of temperature. These are the two largest nanotubes in the 785 nm fluorescence spectra.

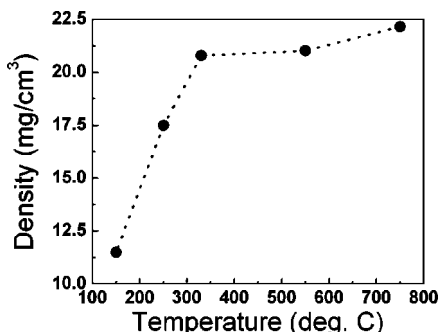


**Figure 5.** Volumetric density of the regrown carpets in  $\text{mg}/\text{cm}^3$ , as a function of the thermal reactivation temperature of the catalyst layer prior to regrowth.

all particle sizes traceable through PL and Raman spectroscopy are reactivated for second growth, and relative intensities of the larger SWNTs in the spectra do not change significantly. This result is consistent with measured carpet densities, shown in Figure 5, which were calculated by weighing the growth substrate before and after growth with a high-precision balance and taking the height and surface area of growth into account. Due to the very thin nature of the carpet grown with room temperature catalyst reactivation, no density measurement was possible. However, the volumetric density measured for the regrown carpet having a catalyst layer annealed at 150 °C was measured to be only 11.5  $\text{mg}/\text{cm}^3$ , which was about one-third of the volumetric densities of the first growth, which were in the range of

$\sim 30\text{--}35 \text{ mg}/\text{cm}^3$ . As the temperature of the catalyst anneal is further increased, the density also increases until  $\sim 330$  °C, where the carpet density does not seem to change from  $\sim 22 \text{ mg}/\text{cm}^3$  as the anneal temperature is further increased. This trend, evident from Figure 5, is in good agreement with observations made in PL measurements and Raman spectroscopy, emphasizing that activation of only the smallest, unstable catalyst particles occurs under thermal annealing experiments in air. In fact, the same trend in Figure 5 is evident by analyzing the results of Figure 4b,c—suggesting this size-dependent activation process is taking place. Also, it should be noted that there is a consistently lower density between carpets grown from the “fully” activated catalyst layer and carpets grown from a fresh catalyst layer. This could be due to the possibility of either (i) the removal of some catalyst by the carpet removal process or (ii) some dynamic catalyst interaction during growth which changes the areal particle density on the surface. It is likely that the latter is the case since we have recently experimentally verified that Ostwald ripening takes place during growth,<sup>31</sup> which in turn leads to a lower catalyst particle nucleation density in a subsequent growth process. As growth rates in “supergrowth” are critically dependent upon the thickness of the catalyst layer (and hence, particle size and density), both of these possibilities are significant factors that could contribute to the inability to recover a carpet with thickness identical to that of the carpet in the first growth with a recycled catalyst layer.

### Multiple Regrowths

In principle, the ability to utilize a 0.5 nm thick catalyst layer for an indefinite number of growth experiments is the driving concept in the ability to regrow from the same substrate. Utilizing the method where the carpet is removed from the growth substrate by simply peeling away the carpet following growth was found to be problematic since the second growth was often slightly nonuniform in height and would not always be cleanly removed from the growth substrate with an adhesive. However, removal of the carpet with an adhesive tape was effective after a procedure that we recently developed to break strong carbon–metal bonds at the SWNT–catalyst interface after growth. This involves a brief 1 min etch with only  $\text{H}_2\text{O}/\text{H}_2$  at an elevated temperature,<sup>23</sup> which will slowly etch amorphous carbon and SWNT ends. Following this treatment, we found that a carpet can be removed from the substrate, subjected to the thermal annealing step described previously, and regrown up to five more times. We found in two isolated experiments that the sixth regrowth (seventh growth) involved matted surface growth of nanotubes, but that no dense aligned structure was obtained. For the purposes of this experiment, we performed growth at lower pressures (1.4 Torr), where the growth rate is slower (due to a lower acetylene partial pressure), and for a shorter growth period of only 15 min, compared to 30 min previously. The reasoning for this is that there is no further need for ultralong growth since the carpet cannot practically

(31) Amama, P. B.; Pint, C. L.; McJilton, L.; Kim, S. M.; Stach, E. A.; Murray, P. T.; Hauge, R. H.; Maruyama, B. *Nano Lett.* **2009**, 9, 44.

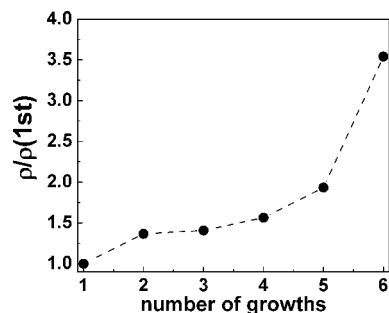


**Figure 6.** Ratio of the resistivity after  $N$  regrows from a recycled catalyst layer and the resistivity of the first carpet grown from the fresh catalyst layer, as a function of the total number of regrowths. Note that an increase in this ratio indicates a thinner and/or less dense regrown carpet.

be imaged via SEM between each growth experiment. In addition, shorter growths were performed since it was unclear in the beginning how many times the carpet would be regrown. To characterize the thickness of the carpet, the carpet was removed from the chip by attachment to a piece of two-sided insulating adhesive tape. Following the multiple regrowths, the resistance of the carpets was measured via a four-point probe setup. The concept of using the resistivity as a gauge of the thickness should be acceptable as long as the carpet is removed under identical conditions each time. Since the resistivity is directly proportional to the thickness of the material, the difference in the measured resistivity from the exact same point on the carpet in successive regrowth cycles can be attributed to the difference in SWNT carpet thickness and/or density. It should be noted from Figure 5 that, even under the optimal conditions for reactivating the catalyst layer, the SWNT density is still slightly lower than that of the first growth. This means that the resistivity measurement treats the total SWNT thickness as an “effective” thickness that is coupled to both the carpet height and density. In this way, the resistivity measurements give insight into changing bulk features of the SWNT array when a detailed height measurement is not obtainable. Figure 6 presents the resistivity, normalized to the resistivity for the first carpet growth, as a function of the number of successive regrowths on the same chip. In each case, after transfer, the catalyst layer was exposed to a 1 min air exposure at a temperature of  $\sim 400^\circ\text{C}$ , as described previously. As shown in Figure 6, the resistivity increases as the number of regrowths continue until the sixth regrowth (or seventh growth), where the growth achieved is no longer carpet growth but rather thin matted growth (the latter is not shown in Figure 6). This result emphasizes a few possibilities that could reside at the heart of some fundamental questions in terms of high-density surface-supported SWNT catalysis. Of particular interest is a comparison of the ratio of conductivity upon successive regrowths, which emphasizes that a rapid increase in resistivity follows the first growth, even though only until the sixth growth does this substantially change. Comparing the second and third growths to that of the first, the effective thickness is  $\sim 65\%$  lower than the first growth. This appears to correspond to the changes in carpet height and density in the second growth as observed previously in Figures 2 and 5, but slightly less change due to less sensitivity of the carpet height under slower growth conditions. The

continuous decrease in the thickness of the carpet as it is regrown emphasizes a process that slowly inactivates some of the catalyst particles, similar to that discussed previously in the context of supergrowth.<sup>32</sup> Under the  $\text{H}_2/\text{H}_2\text{O}$  etch process performed here, TEM measurements of carpets have indicated that there is essentially no Fe particles residing at the ends of the SWNT removed from the growth substrate, meaning that excess Fe is not being lost to the growing SWNT array. To further emphasize this point, carbon densities for carpets grown at 1.4 Torr under the conditions for the multiple regrowth experiments are measured to be  $\sim 60 \text{ mg/cm}^3$ .<sup>21</sup> With assumptions for average catalyst particle size and SWNT diameter being  $\sim 4$  and 3 nm, respectively, our calculations indicate that over half of the catalyst particles must be activated in the growth process to achieve these densities. This is consistent with the estimation that the water-assisted growth technique activates  $\sim 84\%$  of all catalyst particles in growth.<sup>33</sup> As a result, if even one-third of the catalyst was being removed from the  $\text{Al}_2\text{O}_3$  support by the transfer to an adhesive tape, it would be likely that even the second growth would not result in a carpet since this process is highly sensitive to the catalyst thickness and, hence, the areal density of catalyst particles on the surface. However, the difference in carpet height could be due to a dynamic catalyst behavior that is somehow inactivating some of the catalyst particles over time—meaning that irrespective of the reactivation technique, the same particle size distribution and areal density cannot be achieved in a regrowth experiment. This is likely due to one or a combination of a few effects that are currently being understood relevant to highly dense SWNT carpet growth. The first of these is Ostwald ripening, which has recently been shown to be a serious issue in SWNT carpet growth over extended periods of time.<sup>31</sup> In as little as 15 or 30 min, ripening effects clearly change the catalyst particle density on the surface, which could result in a second or third growth from a complete 0.5 nm thick catalyst layer being slightly different in height and/or density. The second possibility is the formation of a stable mixed metal oxide between the Fe and  $\text{Al}_2\text{O}_3$  as the catalyst layer is annealed in air. Although this is also a ripening effect, it will involve Fe–O diffusing into the network of pores that is usually present in a thin, amorphous e-beam  $\text{Al}_2\text{O}_3$  coating, instead of only ripening into larger Fe particles on the surface itself. To better characterize the effect of regrowth in the framework of dynamic catalyst behavior, we performed Raman spectroscopy on the carpets grown in each of the regrowth cycles presented in Figure 6. Raman measurements were taken at two different excitation energies (wavelengths of 633 and 785 nm), with the low-frequency breathing modes and D and G bands of the Raman spectra presented in Figure 7. From this data, a few trends emerge, which give some insight into the nature of the SWNTs grown in successive regrowth cycles. In the first case, the D and G bands ( $\sim 1300$  and  $1590 \text{ cm}^{-1}$ , respectively) do not appear affected by successive regrowths, with

(32) Futaba, D. N.; Hata, K.; Yamada, T.; Mizuno, K.; Yumura, M.; Iijima, S. *Phys. Rev. Lett.* **2005**, 95, 056104.

(33) Futaba, D. N.; Hata, K.; Namai, T.; Yamada, T.; Mizuno, K.; Hayamizu, Y.; Yumura, M.; Iijima, S. *J. Phys. Chem. B* **2006**, 110, 8035.

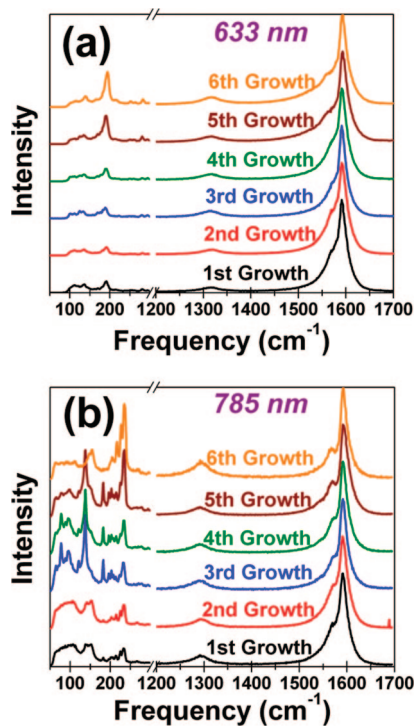


**Figure 7.** Radial breathing modes and D and G bands in Raman spectra for successive carpet regrowths from the same catalyst layer, for (a) 633 nm and (b) 785 nm excitations.

the D/G ratio (hence the “quality”) of the SWNT approximately the same in all regrowth cycles. However, there is a very clear and consistent trend among the lower frequency SWNT diameter-dependent radial breathing modes (RBMs), which are normalized to the G band in Figure 7. Under both excitation wavelengths, the first grown carpet has a significantly greater number of overlaid RBMs close to the cutoff filter for the Raleigh line—similar to that shown in Figure 3a. As the number of successive regrowths increases, the larger diameter RBMs (at the lowest frequency) become less prevalent, whereas the higher frequency RBMs (up to  $250\text{ cm}^{-1}$ ) become stronger relative to the G peak. This means that some process is occurring that is in successive multiple regrowth cycles, leading to the eventual shrinking of the particles and the growth of smaller diameter SWNTs. It should be noted that this would not be the case if the catalyst was static, and the lower density observed in second and successive regrowth cycles was actually due to detachment of the catalyst along with the removed SWNT array, since there should be no reason for selective removal of only the large catalyst particles. Alternatively, the process

of Ostwald ripening should lead to a distribution of shrinking catalytic particles among a distribution of large, growing particles that will likely be inactive under the reaction conditions optimized for SWNT growth. Although further studies isolating dynamic catalyst behavior in these thin catalyst films are currently underway, it should be noted that our limitation to regrow SWNT arrays from a reactivated catalyst layer supporting supergrowth is likely tied to irreversible catalyst migration. In that sense, further techniques to impede the atomic diffusion of alumina-supported catalyst supporting supergrowth of SWNT arrays could be useful not only toward enhancement of the catalyst lifetime but also in creation of robust, static catalyst layers supporting the most efficient process of SWNT supergrowth that can be reactivated and reused multiple times.

### Summary

We present a simple technique to recycle a 0.5 nm thick catalyst layer for the growth of vertically aligned single-walled carbon nanotubes having thicknesses comparable to those of the first growth. In the first case, we emphasize that a termination of all catalyst particles by rapid cooling in a carbon-rich environment allows one to obtain selectivity in a second growth based upon the technique utilized to reactivate the particles. Second, we show that, under conditions where all catalyst particles are reactivated, regrowth of an aligned carpet can be achieved up to five subsequent times from the first growth. On the basis of these results, we discuss the inability to fully regrow a carpet from a recycled catalyst in the framework of dynamic catalyst behavior taking place during the growth process, limiting the ability to renucleate the same SWNT density as in the first growth. This work presents a new technique for achieving selectivity in carpet growth and opens the door for future studies of some concepts that are fundamental to understand in achieving both multiple growths from a recycled catalyst layer and highly efficient extended growth of SWNT carpets.

**Acknowledgment.** The authors acknowledge D. Natelson and group members for use of equipment for catalyst evaporation and J. Tour for use of the Alessa four-point probe. Also, special thanks go to C. Kittrell and H. Schmidt for insightful discussions. This work was partially supported by NASA Grant NNJO6H125A, Air Force OSR Grant FA9550-06-1-0207, and the Lockheed Martin Advanced Nanotechnology Center for Excellence at Rice University.

CM8031626